Earth, Planets and Space
a SpringerOpen Journal

FULL PAPER Open Access

Groundwater, possibly originated from subducted sediments, in Joban and Hamadori areas, southern Tohoku, Japan

Yoko S Togo[1*], Kohei Kazahaya[1], Yuki Tosaki[1], Noritoshi Morikawa[1], Hiroyuki Matsuzaki[2], Masaaki Takahashi[1] and Tsutomu Sato[1]

Abstract

We studied the origin of deep groundwater in the Joban and Hamadori areas in southern Tohoku, Japan, based on δD, $\delta^{18}O$, $^{129}I/I$, $^{36}Cl/Cl$, and ^{3}H concentrations. Deep groundwater was collected from the basement rocks (Cretaceous granite) and from the margin of the Joban sedimentary basin (latest Cretaceous to Quaternary sedimentary rocks deposited on the basement rocks). We sampled groundwater pumped from depths ranging from 350 to 1,600 m in these areas. A hypothetical end-member of deep groundwater was estimated from the relationship between $\delta^{18}O$ and Cl concentrations, and our data reveal a much higher iodine concentration and lower Br and Cl concentrations than found in seawater. The iodine ages inferred from $^{129}I/I$ are quite uniform and are about 40 Ma and $^{36}Cl/Cl$ almost reached the secular equilibrium. The relationship between iodine and Cl can be explained by mixing a hypothetical end-member with meteoric water or seawater. Moreover, the I/Cl ratio increases linearly with increasing water temperature. The water temperature was high in Joban, with a maximum of 78°C at a depth of 1,100 m. The geothermal gradient in the Joban basin is 18°C km^{-1}, and the temperature even at a depth of 3 km in the basin was not high enough to supply thermal water to the sampling sites. Thus, sedimentary rocks in the Joban basin are unlikely to be the source of iodine in the deep groundwater. Several active faults such as the Futaba Fault are developed in and around the studied areas. The Iwaki earthquake occurred 1 month after the 2011 Tohoku-oki earthquake, and normal-fault type surface ruptures formed and discharged hot groundwater in Joban. The deep groundwater we studied probably came up through the basement rocks from greater depths. There are no sedimentary rocks younger than Tertiary age beneath the pre-Cretaceous basement rocks, and the subducted sediments in the Japan Trench are a possible source of iodine in the groundwater. The Joban and Hamadori areas may be an ideal window to look into the water circulation in the forearc of the Tohoku subduction zone.

Keywords: Iodine age; $^{36}Cl/Cl$; Source of iodine; Subducted sediments; Halogen; Joban; Hamadori; Tohoku

Background

The cosmogenic isotopes ^{129}I and ^{36}Cl have been used to investigate the origin of water, such as water found in crustal fluids, oil fields, and geothermal fluids. The half-lives of ^{129}I and ^{36}Cl are 15.7 and 0.3 million years, respectively. According to Muramatsu and Wedepohl (1998), the largest reservoir of iodine in the earth's crust is in ocean sediments. Iodine-rich brine is often generated in forearc and back-arc areas and passive continental margins (Muramatsu et al. 2001; Tomaru et al. 2007a, b, c, 2009a, b; Fehn et al. 2003, 2007a, b; Fehn 2012). Fehn (2012) reported that the iodine-rich fluids in the forearc regions in several subduction zones have iodine ages of about 40 to 60 Ma regardless of the ages of the subducting slab and proposed that the ages represent 'a global pattern of migration of fluids from deep, old layers located in the upper plates.' On the other hand, Muramatsu et al. (2001) proposed that iodine-rich brine produced in Chiba Prefecture, Japan was derived from subducted marine sediments, because the iodine ages are considerably older than the

* Correspondence: yoko-togo@aist.go.jp
[1]Institute of Earthquake and Volcano Geology, National Institute of Advanced Industrial Science and Technology (AIST), 1-1-1 Higashi, Tsukuba, Ibaraki 305-8567, Japan
Full list of author information is available at the end of the article

Springer

© 2014 Togo et al.; licensee Springer. This is an Open Access article distributed under the terms of the Creative Commons Attribution License (http://creativecommons.org/licenses/by/2.0), which permits unrestricted use, distribution, and reproduction in any medium, provided the original work is properly credited.

ages of the host formations. They also suggested that the recycling of iodine could occur in forearc areas and that this process should be considered for the marine iodine budget. Iodine is a biophilic element and is strongly enriched in organic matters (Elderfield and Truesdale 1980). Sediments on continental margins are enriched with iodine because of higher organic content and higher depositional rates than in open oceans (Martin et al. 1993; Fehn et al. 2007b). Thus, subducted marine sediments in the open ocean may not provide iodine to the forearc regions. However, Premuzic et al. (1982) and Klauda and Sandler (2005) report fairly high organic carbon in surface sediments over a wide area of the northwestern margin of the Pacific Plate (several times as high as in open oceans), even far east of the outer rise in the Japan Trench. Thus, we do not consider that 'subducted sediments' are excluded as possible iodine sources, at least in the Tohoku subduction zone.

We searched for the origin of iodine in deep groundwater collected from hot springs in the Joban and Hamadori areas in southern Tohoku, Japan, by measuring the $^{129}I/I$, $^{36}Cl/Cl$, δD, $\delta^{18}O$, and ^{3}H concentrations. Most of our samples are hot spring water pumped from the Cretaceous granite (Figure 1a). There are no sedimentary rocks (possible sources of iodine) younger than the Tertiary beneath the granitic basement, and geologically this is a unique aspect of the study area. We also sampled groundwater pumped from sedimentary rocks at the margin of the Joban sedimentary basin where the latest Cretaceous to Quaternary sedimentary sequences were deposited on the basement rocks (Figure 1b; Inaba et al. 2009). Natural gas was produced in the Joban basin until 2007 at Iwaki-oki gas field, located at the central part of the basin. This paper compares deep groundwater with different host rocks and discusses the source of iodine contained in the water.

Both Joban and Hamadori are located along the Pacific coast of Ibaraki and Fukushima Prefectures in southern Tohoku where several active faults, including the Futaba Fault, are distributed (Figure 1a; The Research Group for Active Faults of Japan 1991; GeomapNavi 2014). The temperature of the hot spring water we sampled in Joban is high, with a maximum of 78°C at a depth of 1,100 m, probably because the areas are tectonically active (there are no nearby active volcanoes). Moreover, the 11 April 2011 Iwaki earthquake (Mw 6.6), an aftershock of the 2011 Tohoku-oki earthquake (Mw 9.0), occurred in Iwaki City (Fukushima et al. 2013), and the surface ruptures and crustal deformation with normal displacements formed along the Itozawa and Yunodake Faults (Kobayashi et al. 2012; Toda and Tsutsumi 2013) near our sampling sites in Joban (Figure 1a). The earthquake discharged thermal water in the city with a flow rate reaching about 10,000 m^3 day^{-1} in May 2011 (Sato et al. 2011; Kazahaya et al. 2013). The massive discharge of water suggests that the tectonic activity promotes upward movement of deep groundwater in the areas. We examine the origin of deep groundwater in both Joban and Hamadori areas in view of their geological and tectonic settings, as well as their isotope compositions.

Methods

Geological settings and water samples

The Joban and Hamadori areas are located in the northeastern part of Ibaraki Prefecture and the southeastern part of Fukushima Prefecture, Japan (Figure 1a). The Joban sedimentary basin is located offshore and consists of a nearly continuous sequence of sedimentary rocks of about 5,000-m maximum thickness that has been deposited on the basement rocks since late the Cretaceous (Figure 1b; Inaba et al. 2009). The Maastrichtian-Paleogene coals and coaly mudstones are the most likely sources of natural gas (Iwata et al. 2002). Inaba et al. (2009) demonstrated that the Cretaceous argillaceous rocks in the basin can potentially generate petroleum if there is abundant marine organic matter deposited in an anoxic environment. The Abukuma belt is located west of the Joban basin and consists of metamorphic rocks and Cretaceous granite (e.g., Hiroi et al. 1998). The Hatagawa Fault is considered to be the boundary between the Abukuma and Southern Kitakami Belts (e.g., Tomita et al. 2002). However, we treat basements rocks in the two belts and those beneath the Joban basin as 'pre-Cretaceous basement rocks' in this study. Coastal areas, including our sampling sites, are covered with thin Tertiary sedimentary rocks and Quaternary sediments (green and white areas, respectively, in Figure 1a; GeomapNavi 2014). Those sedimentary rocks cover the pre-Cretaceous basement rocks and constitute the western margin of the Joban basin. Active faults are shown with red lines in Figure 1a.

We sampled deep groundwater at ten hot spring wells in areas A and B in Hamadori, and in areas C and D in Joban, and river water at two locations in area E in Hamadori (Figure 1a; numbers 1 to 12 indicate sampling localities). We also use the sampling localities as sample numbers (Table 1, column 2). Hot spring drill holes penetrate through surface sediments into granitic basement in areas A, C, and D and into sedimentary rocks of the Joban basin in area B. The depth of the basement granite was about 800 m in a drill hole very close to locality 2 (Yanagisawa et al. 1989) and 1,100 to 1,200 m at the western part of Fukushima First and Second Nuclear Power Plant sites (FNPP1 and FNPP2 in Figure 1a; Tokyo Electric Company 2012). The pumping depths in area A are 1,200 to 1,600 m (Table 1, column 3), and our groundwater samples in area A were collected from the upper part of the granite basement. According to the information on drilling at a hot spring (locality 5), the hot spring water in area B is pumped from the Oligocene

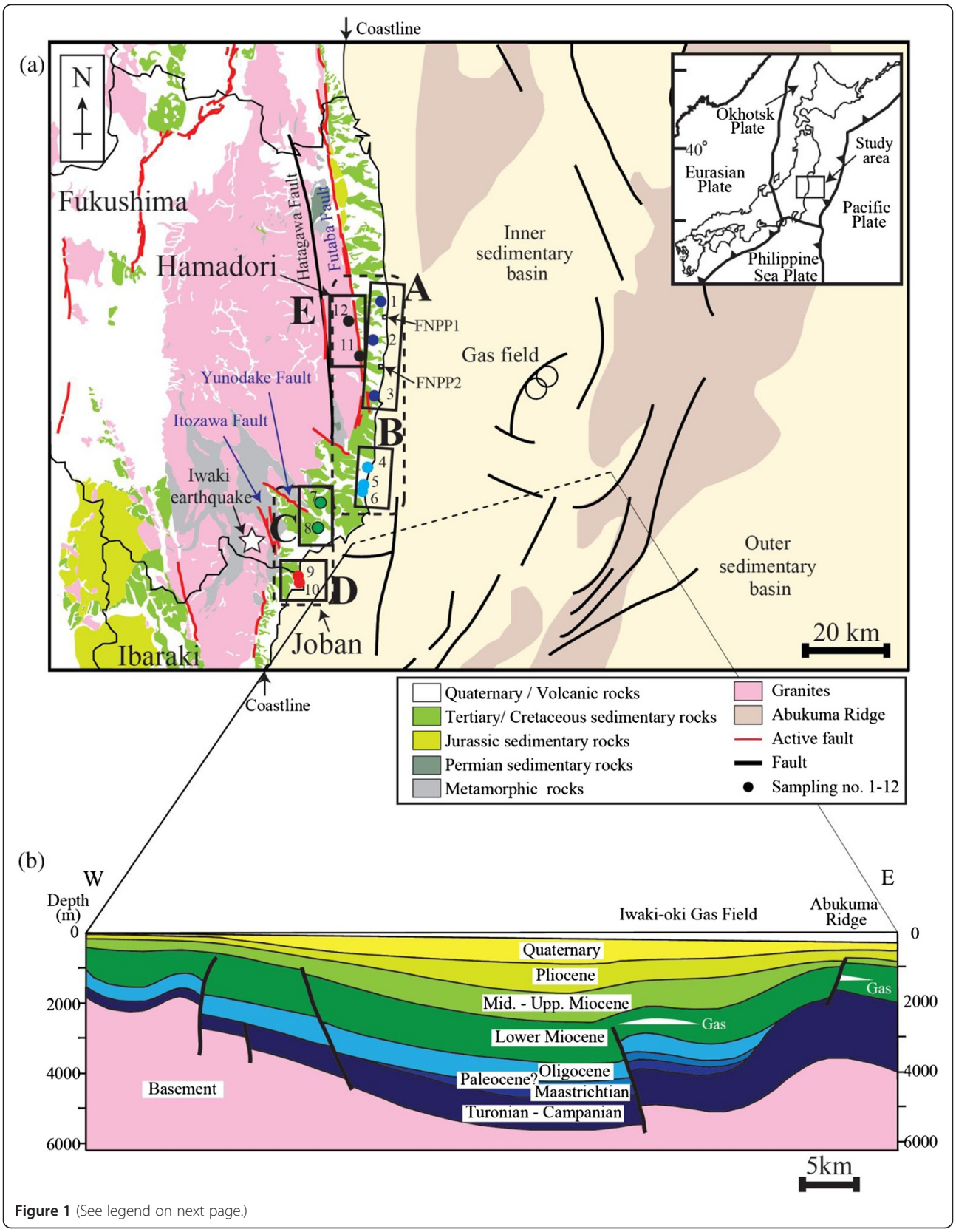

Figure 1 (See legend on next page.)

(See figure on previous page.)
Figure 1 Geological setting. (a) A simplified geological and geographical map of the Fukushima-Ibaraki area and sampling localities 1 to 12; an inset figure shows the location of the study area (box), southern Tohoku, Japan, with plate configurations. On-land geological map is simplified from GeomapNavi (2014). Miocene volcanic rocks are widely distributed in the Abukuma belt but are not shown in **(a)** to highlight the basement rocks. The sampling area is divided into areas A to E, and an asterisk indicates the epicenter of the Iwaki Earthquake (Japan Meteorological Agency 2011). The Fukushima First and Second Nuclear Power Plants are located at FNPP1 and FNPP2, respectively, in area A. **(b)** A schematic geologic cross section across the offshore Joban basin after Inaba et al. (2009). Ages of sediments are given on each formation.

Iwaki formation in the landward margin of the Joban basin (*cf.* Figure 1b). The drilling depths for hot springs in area C are not clear, but we obtained information at a hot spring facility that the water is pumped from the basement granite. The depth of the basement metamorphic rocks is about 800 m in area D, but those rocks are thermally metamorphosed and may be close to granite (Kasai 2008). Thus, we consider that the groundwater in area D was sampled from metamorphic or granitic basement rocks. However, groundwater sampled at a depth of 350 m was collected from sedimentary rocks in the Joban basin.

We sampled the hot spring water pumped from the depths shown in the third column of Table 1. Because of the limited sample volumes during the first sampling,

Table 1 List of water samples and their chemical and isotopic compositions

Area	Sampling number	Depth (m)	Sampling date	Temperature (°C)	Chlorine (mM)	Bromine (μM)	Iodine (μM)	^{129}I/I ratio ($\times10^{-15}$)	I age (Ma)	^{36}Cl/Cl ratio ($\times10^{-15}$)	^{3}H (TU)[a]	δD (‰)	δ^{18}O (‰)
A	1	1,600	10 December 2003	31.6	374	472	20	388 ± 25	31	6.1 ± 1.1	<0.53[b]	−28	−4.3
	2	1,500	10 December 2003	41.1	285	355	69	218 ± 12	44	-	-	−32	−3.2
			16 March 2010	38.5	270	380	-	-	-	15.7 ± 2.0	-	−33	−3.5
	3	1,200	10 December 2003	40.4	335	575	49	255 ± 18	40	22.9 ± 2.4	<0.40[b]	−25	−3.2
B	4	-	3 July 2007	17.6	34.4	56.3	-	-	-	2.1 ± 0.8	<0.04[c]	−50	−7.6
			20 November 2012	16.1	37.1	53.0	3.0	281 ± 25	38	-	-	−49	−7.7
	5	1,500	3 July 2007	44.1	434	695	-	-	-	6.5 ± 1.4	<0.04[c]	−13	−3.2
			20 November 2012	44.2	392	577	44	247 ± 23	41	-	-	−14	−3.4
	6	1,500	3 July 2007	39.3	79.2	120	-	-	-	7.1 ± 1.2	0.12 ± 0.02[c]	−36	−6.0
			20 November 2012	38.6	57.9	70.7	6.4	232 ± 36	42	-	-	−37	−6.5
C	7	-	3 July 2007	58.8	17.6	27.5	-	-	-	16.5 ± 4.9	1.74 ± 0.05[c]	−47	−7.3
			28 April 2011	58.3	19.8	29.4	-	-	-	-	1.28 ± 0.04[c]	−47	−7.4
			23 October 2012	57.9	18.0	25.6	3.1	5840 ± 132	-	-	-	−47	−7.5
	8	-	18 May 2011	56.1	38.3	56.3	-	-	-	27.8 ± 2.7	0.63 ± 0.03[c]	−44	−6.9
			22 February 2012	62.4	35.7	51.3	-	-	-	36.5 ± 3.1	0.6 ± 0.1[d]	-	-
			23 October 2012	63.8	34.2	50.1	6.0	1790 ± 80	-	-	-	−45	−7.2
D	9	880	11 December 2003	35.7	203	319	57	257 ± 14	40	7.3 ± 1.1	<0.41[b]	−25	−3.5
	10	1,100	11 December 2003	77.8	185	287	-	-	-	7.3 ± 1.2	<0.53[b]	−27	−3.8
			19 December 2012	76.2	187	278	43	312 ± 13	36	-	-	−27	−3.8
		1,100	11 December 2003	64.5	211	324	59	239 ± 31	42	8.5 ± 1.4	<0.53[b]	−24	−3.3
			19 December 2012	67.3	220	336	49	199 ± 11	46	-	-	−25	−3.4
		350	11 December 2003	38.5	41.4	66.3	-	-	-	20.3 ± 2.2	<0.34[b]	−44	−7.0
			19 December 2012	36.9	44.7	70.4	7.8	303 ± 15	36	-	-	−45	−7.1
E	11	River	19 May 2008	11.6	0.17	-	-	-	-	58.6 ± 4.3	-	-	-
	12	River	19 May 2008	13.8	0.12	-	-	-	-	116.0 ± 7.4	-	-	-
Seawater[e]					550	840	0.44						
Meteoric water[f]					0.28	0.48	0.05						

[a]^{3}H concentrations in groundwater samples were measured using liquid scintillation analyzer ([b]Packard, 3100TR, [c]PerkinElmer 1220 Quantulus (Morgenstern and Taylor 2009), [d]LSC-LB5); [e]elemental concentration data for seawater were taken from Geochemical Earth Reference Model (2014); [f]elemental concentration data for meteoric water were taken from Tagami and Uchida (2006). Sampling localities for the second column are shown in Figure 1a. The third to fifth columns give depths from which hot groundwater was pumped out, date of sampling, and water temperature at the time of sampling.

we collected more samples later. However, the δD, $\delta^{18}O$, elemental concentration, and temperature for these locations showed small temporal variations even before and after the 2011 Tohoku-oki earthquake, so we treated the data collected at different times in the same way. Table 1 also summarizes the sampling dates, chemical data, and estimated iodine age.

Methods for chemical and isotope analyses

Hydrogen and oxygen isotope compositions (δD and $\delta^{18}O$) were measured by mass spectrometry or cavity ring-down spectroscopy. The CO_2/H_2O equilibrium method and the H_2 reduction method using Cr metal were used for the analyses of oxygen and hydrogen isotopes, respectively (mass spectrometers, Delta Plus and Delta V advantage; Thermo Fisher Scientific Inc., Waltham, MA, USA). The precision of these measurements was ±0.1‰ for $\delta^{18}O$ and ±1‰ for δD. Oxygen and hydrogen isotope compositions are presented in the δ notation in per mille relative to the Vienna Standard Mean Ocean Water (V-SMOW). The precision for the analysis by cavity ring-down spectroscopy (Picarro cavity ring-down spectrometer L2120-i; Picarro Inc., Santa Clara, CA, USA) was ±0.1‰ for $\delta^{18}O$ and ±0.6‰ for δD. For the analysis of I, Br, and Cl, water samples were filtered using 0.45-μm membrane filters. Iodine concentrations in the groundwater samples were determined by inductively coupled plasma mass spectrometry (Agilent 7700; Agilent Technologies, Santa Clara, CA, USA). Groundwater samples were diluted with 0.5 wt.% tetramethylammonium hydroxide and spiked with Re as an internal standard. Cl and Br concentrations were determined by ion chromatography (Dionex, DX-500; Thermo Fisher Scientific Inc., Waltham, MA, USA).

To determine iodine age, $^{129}I/I$ ratios of deep groundwater were measured by accelerator mass spectrometry (AMS), using the sample preparation scheme developed by Muramatsu et al. (2008). Groundwater samples were purified by solvent extraction and back extraction using CCl_4. Purified iodine was precipitated as AgI by adding $AgNO_3$, and the AgI precipitate was washed with ultrapure water and NH_4OH. The supernatant was removed after centrifugation, and the AgI was freeze-dried. The $^{129}I/I$ ratio was measured at the Micro Analysis Laboratory Tandem Accelerator (MALT) at the University of Tokyo, following the method detailed in Matsuzaki et al. (2007).

The $^{36}Cl/Cl$ ratios of the samples were measured by AMS at the Australian National University (Fifield et al. 2010) or at the Purdue Rare Isotope Measurement Laboratory (PRIME Lab), Purdue University, USA (Sharma et al. 2000) to investigate the age of Cl. The samples were acidified with concentrated HNO_3 to precipitate AgCl by adding $AgNO_3$. The AgCl precipitate was separated by centrifugation and dissolved in NH_4OH. The SO_4^{2-} was precipitated as $BaSO_4$ by adding a saturated $Ba(NO_3)_2$ solution to remove isobaric interference from ^{36}S, and the $BaSO_4$ precipitate was eliminated by filtration. The AgCl was precipitated again and separated by centrifugation before drying. Sample numbers 11 and 12 were prepared following the procedures described in Tosaki et al. (2011), and their $^{36}Cl/Cl$ were measured with the AMS system at the Tandem Accelerator Complex, University of Tsukuba (Sasa et al. 2010). Isotope ^3H is one of the most commonly employed radioisotopes used to identify the presence of a modern water component. The ^3H concentrations in groundwater were measured after electrolytic enrichment, using a liquid scintillation analyzer (Packard 3100TR, PerkinElmer 1220 Quantulus (PerkinElmer Inc., Waltham, MA, USA), or LSC-LB5 (Hitachi Aloka Medical, Ltd., Mitaka, Tokyo, Japan).

Results

Isotope compositions and the estimation of hypothetical end-members

Figure 2 exhibits isotope and chemical compositions of groundwater from areas A to D. The d parameter ($d = \delta D - 8\delta^{18}O$) after Dansgaard (1964) is mostly in the range of 15 to 20 for the Abukuma area (Takahashi et al. 2004) and 10 to 12 for the Kanto Plain (Inamura and Yasuhara 2003). The $\delta^{18}O$ values of several samples collected from the A and D areas are slightly heavier than the meteoric water lines using d values of 10 and 20 (MWL in Figure 2a). The positive shift of $\delta^{18}O$ can be explained by isotopic exchange between water and rock (Figure 2a), and this characteristic is often found in connate water such as oil field brine (Clayton et al. 1966; Mahara et al. 2012). The relationship between the Cl and $\delta^{18}O$ of the samples from areas A and B cannot be explained by simple mixing between meteoric water and seawater (Figure 2b). The Cl concentration of the hypothetical end-member was determined to be 361 mM by extrapolating the best-fit line for the data from area D to 0‰ of $\delta^{18}O$. Higher Cl in some data from areas A and B may be due to the mixing of seawater through the sedimentary rocks.

The concentration of Br correlates well with that of Cl (correlation coefficient, $R = 0.99$), suggesting simple mixing between the meteoric water and seawater (Figure 2c). On the other hand, the iodine concentration in deep groundwater is much higher than in meteoric water and seawater (Figure 2d). The highest iodine concentration was approximately 150 times higher than the seawater value. The I and Br concentrations of the hypothetical end-members were inferred from the mixing lines between the meteoric water and data from area D (asterisks in Figure 2c,d), using the Cl concentration at the end-member in Figure 2b. The Br and Cl concentrations of the hypothetical end-members are diluted (Figure 2c). The I and Cl concentrations for some samples from areas A and B can be explained by the mixing

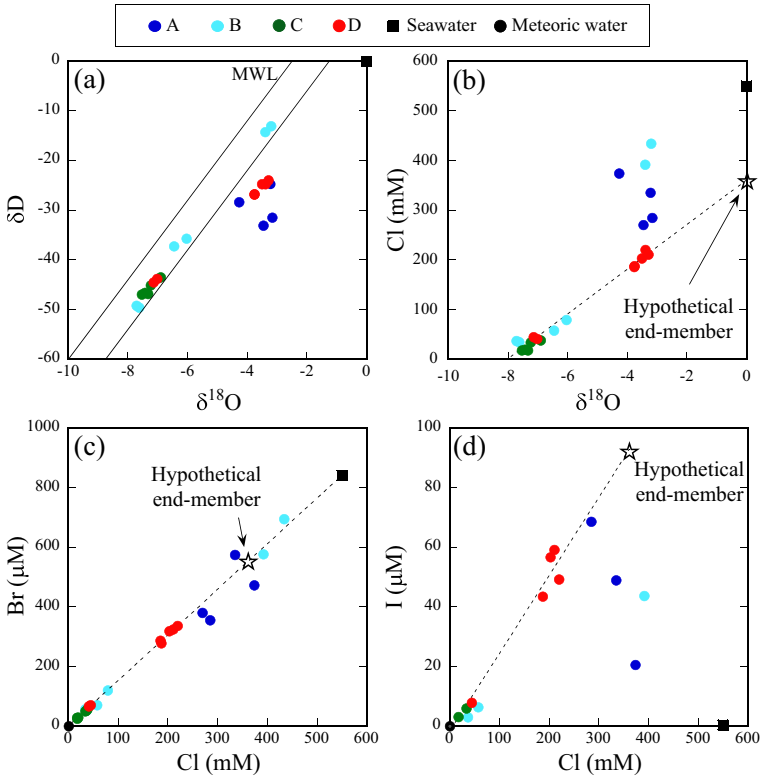

Figure 2 Relationships between δD, $\delta^{18}O$, Cl, Br, and iodine in groundwater samples. MWL, meteoric water lines with *d* parameters of 10 and 20. Relationships between **(a)** δD and $\delta^{18}O$, **(b)** Cl concentration and $\delta^{18}O$, **(c)** Br and Cl concentrations, and **(d)** iodine and Cl concentrations.

of the hypothetical end-member (asterisk), meteoric water (filled black circle), and seawater (filled black square), except for two samples with low I and Cl concentrations (Figure 2d). In contrast, those for samples from areas C and D in granitic basement can be explained by the mixing of the hypothetical end-member with meteoric water.

Figure 3 exhibits an interesting correlation among the four areas. The I/Cl increases with increasing temperature of deep groundwater, and the ratio and temperature for areas C and D are much higher than for areas A and B.

Age of I estimated from $^{129}I/I$

We estimated the ages of I in the deep groundwater from the measured $^{129}I/I$ of the water samples. Three gray curves in Figure 4 indicate mixing lines, on logarithmic scales, of the water sample with the highest iodine content (number 2 in Table 1), with the anthropogenic meteoric water, pre-anthropogenic seawater, and pre-anthropogenic meteoric water. Snyder and Fehn (2004) report five $^{129}I/I$ values of anthropogenic meteoric water in Japan that vary widely from 2.0×10^{-10} to 7.9×10^{-9} (cross marks in Figure 4a). We did not measure the $^{129}I/I$ of meteoric water, using their lowest value instead, because it falls on the mixing line. To draw the other two mixing lines, we used a reported value of $^{129}I/I$ (1.5×10^{-12}) for the

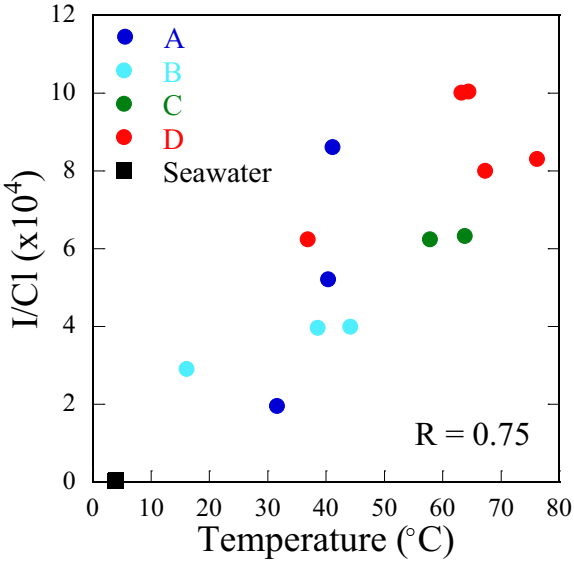

Figure 3 Relationship between I/Cl weight ratio and temperature of deep groundwater. Seawater temperature (4°C) was calculated as an annual average of seawater off Fukushima Prefecture, at a depth of 400 m in 2013, using data from the Japan Meteorological Agency (2013).

pre-anthropogenic water (Moran et al. 1998; Fehn et al. 2007a) and iodine concentrations of Abukuma River near the sampling site after Tagami and Uchida (2006) and typical seawater (Table 1). The results for the samples from areas A, B, and D can be explained by the mixing of the water with the highest iodine content with the pre-anthropogenic meteoric and seawater (Figure 4). This is consistent with the relationship between iodine and Cl in Figure 2d. The two samples from area C have higher ^{129}I/I values (green filled circles in Figure 4) than the pre-anthropogenic water. They also contained detectable ^{3}H (half-life: 12.32 years) of 1.28 ± 0.04 and 0.6 ± 0.1 TU, where 1 TU is defined as the ratio of 1 tritium atom to 10^{18} hydrogen atoms. Thus, the water from area C is likely to have mixed with shallow groundwater containing anthropogenic ^{129}I, and we did not use them for the age determination. Sample number 6 from area B contained detectable ^{3}H, but no significant contamination of anthropogenic ^{129}I was recognized.

Iodine age was calculated by the decay equation:

$$R_{obs} = R_i e^{-\lambda_{129} t} \quad (1)$$

where R_{obs} is the measured ^{129}I/I, R_i is the initial ^{129}I/I (assumed to be 1.5×10^{-12}), and λ_{129} is a decay constant of 4.41×10^{-8} year^{-1} (Fehn 2012). Most samples have a ^{129}I/I value of (0.2 to 0.3) $\times 10^{-12}$ irrespective of the iodine concentration and I/Cl ratio (Figure 4b), which gives iodine ages of 36 to 46 Ma. We neglect fissiogenic ^{129}I produced by spontaneous fission of ^{238}U because its influence is small (Fehn et al. 2000; Tomaru et al. 2007a, c, 2009a, b). The homogeneity of iodine age (39 ± 4 Ma) suggests that the source of iodine is limited.

Secular equilibrium of ^{36}Cl of the deep groundwater

We calculated the ^{36}Cl/Cl ratios at secular equilibrium between the production and decay of ^{36}Cl using the chemical compositions of the host rocks (Additional file 1: Table S1). Figure 5 shows the relationships between ^{36}Cl/Cl and 1/Cl for the samples from the four areas. The secular equilibrium ^{36}Cl/Cl (R_e) can be calculated by the following equation (Andrews et al. 1986; Snyder and Fabryka-Martin 2007; Morikawa and Tosaki 2013):

$$R_e = \frac{\varnothing \sigma_{35Cl}}{\lambda_{36}} N \quad (2)$$

The thermal neutron absorption cross section of ^{35}Cl (σ_{35Cl}) is 43.6×10^{-24} cm^2, the decay constant (λ_{36}) of ^{36}Cl is 2.3×10^{-6} year^{-1}, and the isotopic abundance (N) of ^{35}Cl is 0.7577. The thermal neutron flux ($\varnothing$), in neutron per square centimeter per year, was estimated from the whole-rock major and trace element compositions of various sedimentary rocks and granitic rocks collected in this area (Additional file 1: Table S1; Morikawa and Tosaki 2013). The secular equilibrium ^{36}Cl/Cl (R_e) are calculated and plotted as horizontal dashed lines for areas A, C, and D with granitic basement ($R_e = (1.77 \pm 0.82) \times 10^{-14}$), and as horizontal solid lines for area B with sedimentary rocks ($R_e = (9.87 \pm 3.10) \times 10^{-15}$) in Figure 5. The equilibrium between ^{36}Cl production and decay is established in approximately 1.5 Ma (Andrews et al. 1986). The ^{36}Cl/Cl values of most of our samples are plotted at or near the horizontal lines, and they have nearly reached secular equilibrium. Note that a state of true equilibrium may not be attained with a single, specific type of host rock in a strict sense, possibly leading to some uncertainty in the above interpretation. Overall, the deep groundwater in the Joban and Hamadori area has not been affected by modern seawater, even though the areas are located near the coast.

Discussion

The origin of iodine

We discuss the possible sources of iodine in the deep groundwater collected at ten hot springs in the Joban and Hamadori areas and implications for water circulation in the Tohoku subduction zone. The measured concentrations of iodine in the groundwater were much higher than in seawater (Figure 2d), whereas Cl and Br concentrations were lower than in seawater (Figure 2b,c). Iodine is strongly bound to organic matter under marine conditions (Elderfield and Truesdale 1980) and is released during the diagenesis of organic material to form natural water enriched in iodine, such as oil field brines and pore waters in marine sediments (e.g., Tomaru et al. 2009a, b; Fehn 2012). Previous papers report that Br is also released during decomposition of organic materials (Tomaru et al. 2007c, 2009b), but the enrichment of Br did not occur in the deep groundwater we studied. A possible reason for this is that the release rate of iodine from organic matter is higher than that of Br (Tomaru et al. 2009b). The iodine of about 40 Ma in age in the deep groundwater must have derived from sedimentary rocks, and there are two possible sources, the Joban sedimentary basin, east of the hot springs where we did the sampling (Figure 1), and the subducted marine sediments from the Japan Trench beneath Tohoku, as discussed below.

We do not exclude the Joban basin as a possible iodine source, but we consider it unlikely for the following three reasons: (1) The lower Miocene formation in the Joban basin contains a thick layer of fine to coarse sandstone and conglomerate, which comprise a gas reservoir, and the iodine-containing water may have migrated up along the formation towards the hot spring wells where we sampled the deep groundwater (Figure 1b). However, the geothermal gradient at the Joban gas field (Figure 1a) is 18°C km^{-1} (Tanaka et al. 2004), and the expected

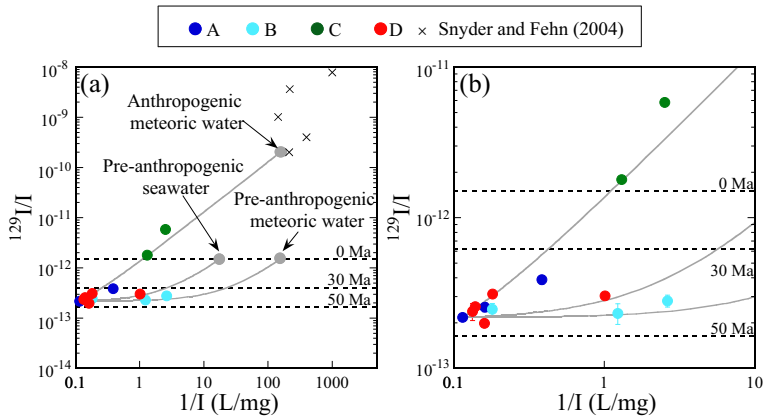

Figure 4 Mixing diagrams in the ^{129}I/I versus 1/I space (a) and (b) is the enlarged portion of (a). Lines indicate mixing between pre-anthropogenic meteoric water, seawater, and anthropogenic meteoric water with the highest I samples. Ages above the dashed lines indicate iodine ages, as determined from Equation 1.

temperature at maximum depth (approximately 3 km) for the formation is about 70°C. This is lower than the temperature of the groundwater in area D (close to 80°C maximum, Figure 3), and the high temperature of the groundwater cannot be explained by the water in the Joban basin as its source (there is no heat source such as a volcano in the sampling area). (2) Deep groundwater samples in areas A, C, and D were collected in basement granitic rocks, but the temperature of the water is higher than

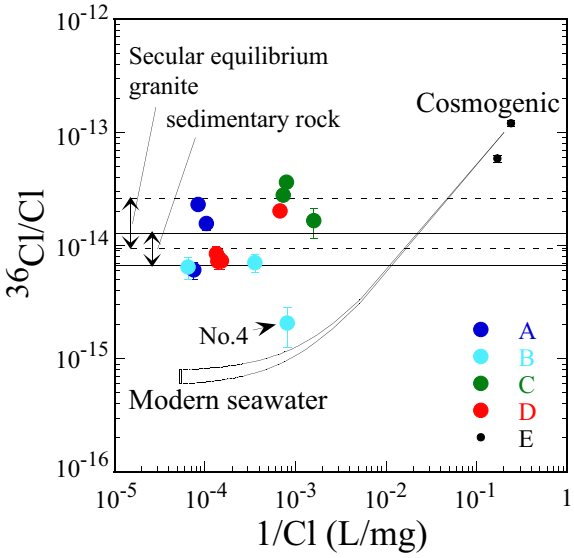

Figure 5 Mixing diagrams in the ^{36}Cl/Cl versus 1/Cl space. Horizontal lines indicate the secular equilibrium (R_e) of ^{36}Cl/Cl for granite and sedimentary rocks, estimated from the chemical compositions of host rocks (Additional file 1: Table S1). Black-filled circles give the ^{36}C/Cl and 1/Cl values of two river water samples collected in area E, representing the cosmogenic end-member. Lines indicate mixing between cosmogenic and modern seawater values after Fifield et al. (2013).

that of water from the Joban sedimentary rocks in area B (Figure 3). Presumably, hot groundwater from depths comes up close to the surface in areas A, C, and D through the basement rocks. (3) Several active faults are developed in the sampled and neighboring areas, and surface ruptures formed along the Itozawa and Yunodake Faults during the 2011 Iwaki earthquake (red lines in Figure 1a; The Research Group for Active Faults of Japan 1991; Toda and Tsutsumi 2013). This earthquake discharged thermal water in Iwaki City for at least 2 years (Sato et al. 2011; Kazahaya et al. 2013). The earthquake was of a normal-fault type with complex ruptures and aftershocks extending to a depth of almost 15 km (Fukushima et al. 2013). The active tectonics of the sampled areas must have promoted discharge of deep groundwater from depths through the basement rocks, rather than from the Joban basin. The geothermal gradients in the Joban-Hamadori areas are 24°C km^{-1} to 33°C km^{-1} (Tanaka et al. 2004), but the temperature of the hot spring water is higher than the geothermal gradient in about half of the hot springs where we sampled groundwater (Figure 3).

The deep groundwater we sampled came through the pre-Cretaceous basement rocks. Thus, the geological situation in our study area is different from those studied by Fehn et al. (2003) and Tomaru et al. (2007b, 2009a), who sampled pore waters in sediments on the continental slopes in the Nankai Trough and off the Shimokita Peninsula, northern Japan. In our study area, it is hard to expect sedimentary rocks younger than 40 Ma beneath the pre-Cretaceous basement. The subduction zone in the Japan Trench is regarded as a classical erosion boundary and sediments on the continental slope deposited on Cretaceous rocks (von Huene and Culotta 1989). Moreover, von Huene and Lallemand (1990) proposed that the subduction of seamounts would play an important role in the

erosion and estimated that the rate of tectonic erosion at a subducting plate boundary is comparable to the rate of sediment accretion. Thus, rocks constituting the upper plate in the Japan Trench are unlikely to be accreted large-scale sedimentary rocks, younger than the Cretaceous. However, a small-scale accretionary prism is developed throughout the Japan Trench, and a thin interplate layer, possibly composed of sedimentary rocks, is recognized along the plate interface down to a depth of almost 20 km (Figure 6; Tsuru et al. 2002; Miura et al. 2003). The types of subducting sediments are unclear in the southern part of the Japan Trench, but DSDP drilling at leg 56 site 436 revealed that incoming sediments are mostly pelagic sediments of a few hundred-meter thickness and of Miocene to Pliocene in age (about 20 to 2 Ma) (The Shipboard Scientific Party 1980; Kimura et al. 2012, Figures two panel b and four). Chester et al. (2013) report very similar sediments beneath the coseismic fault during the Tohoku-oki earthquake in the J-FAST drill cores in the Japan Trench. Moreover, sediments in the western Pacific Ocean near the Japanese Islands contain organic carbon of 0.5 to 1.0 wt.%, much higher than in sediments in the Pacific Ocean away from land (Premuzic et al. 1982, Figure one; Klauda and Sandler 2005, Figure three). We thus consider that subducted sediments in the Japan Trench are possible sources of iodine in the deep groundwater in the Joban-Hamadori areas.

Implications for water circulation in subduction zones

The subducted sediments undergo a series of dehydration reactions (Figure 6). Kimura et al. (2012) showed using a new temperature calculation that the opal A-CT-quartz transition and smectite-illite transition occur at the plate interface between 40 to 80 and 80 to 120 km, respectively, landward of the Japan Trench (Figure 6). The hypothetical end-member determined in this study shows higher iodine and lower Cl concentrations than seawater. The dehydration of hydrous minerals releases water and dilutes the Cl concentration in pore fluid; hence, the source of deep groundwater is probably deeper than those dehydration depths. Moreover, the isotope and trace element composition revealed the involvement of sediments in the generation of island-arc magma in northeast Japan (Shibata and Nakamura 1997), strongly suggesting that the subduction component is carried to depths exceeding 150 km. The mantle wedge may be serpentinized, in view of a result of seismic wave tomography (Figure 6; e.g., Miura et al. 2003), also suggesting the release of a large amount of water beneath the mantle wedge.

Microseismicity has been recognized in the mantle wedge to form the aseismic front (AF in Figure 6) roughly below the coastline (Yoshii 1975, 1979). Thus, the overriding plate off the coast of the study area is characterized by the mantle wedge and basement crust, both seismogenic, and slope sediments covering the basement rocks. Shale is very impermeable, particularly in the direction normal to the bedding plane (Kwon et al. 2004a, b and references therein), and even the clay-bearing fault gouge has a permeability of as low as 10^{-17} to 10^{-22} m^2 (Faulkner and Rutter 2000). Therefore, fluids probably cannot easily penetrate through the slope sediments containing low-permeability shale, although we are not aware of any permeability data on the slope sediments in the Tohoku subduction zone, whereas fractured basement rocks have much higher permeability (e.g., 10^{-15} to 10^{-18} m^2 in the case of cataclasite along the Median Tectonic Line; Uehara and Shimamoto 2004). Hence, the overall permeability structures might have promoted fluid flow through fractured basement rocks from the subducting plate towards the coastline.

In addition, Imanishi et al. (2012) recognized that normal-fault type earthquakes had occurred locally in the Joban and Hamadori areas even before the 11 March 2011 Tohoku-oki earthquake, despite the stress field in Tohoku being dominated by E to W compression. The 11 April 2011 Iwaki earthquake and associated surface ruptures were of normal-fault type (Fukushima et al. 2013; Toda and Tsutsumi 2013). Moreover, Imanishi et al. (2012) found a clear normal-fault type earthquake sequence extending from the subducting plate to the aftershock area and called it a branching fault (shown by a thick red line in Figure 6; small gray circles are aftershocks traced along profile EE' in Figure four of their paper). The study area is the only place in the focal area of the Tohoku-oki earthquake where aftershocks are distributed continuously from the subducting plate to the coastal area of Tohoku. The branching fault is a broad zone of microseismicity and probably acted as a fluid conduit from the subducting plate to the study area. The discharge of a large amount of thermal water after the Iwaki earthquake (Sato et al. 2011; Kazahaya et al. 2013) strongly suggests that the earthquakes promote upward movement of deep groundwater in the areas. If the deep groundwater in the study area came out through the broad branching fault zone, the path of the water along the fault would be about 80 to 90 km. The ages of the incoming sediments range from 2 to 20 Ma, as reviewed above, and it takes about 2 Ma for the sediments to reach the intersection of the subducting plate and the branching fault. Thus, the iodine age of about 40 Ma gives 2 to 5 mm $year^{-1}$ as the average speed of H_2O migration in the overlying plate. The low speed may imply that fractures are sealed rapidly, and fault valve behavior (Sibson 1992, 2013) controls the fluid flow. Whether an average velocity of a few to several millimeters per year is appropriate or not needs a test from additional study in the future.

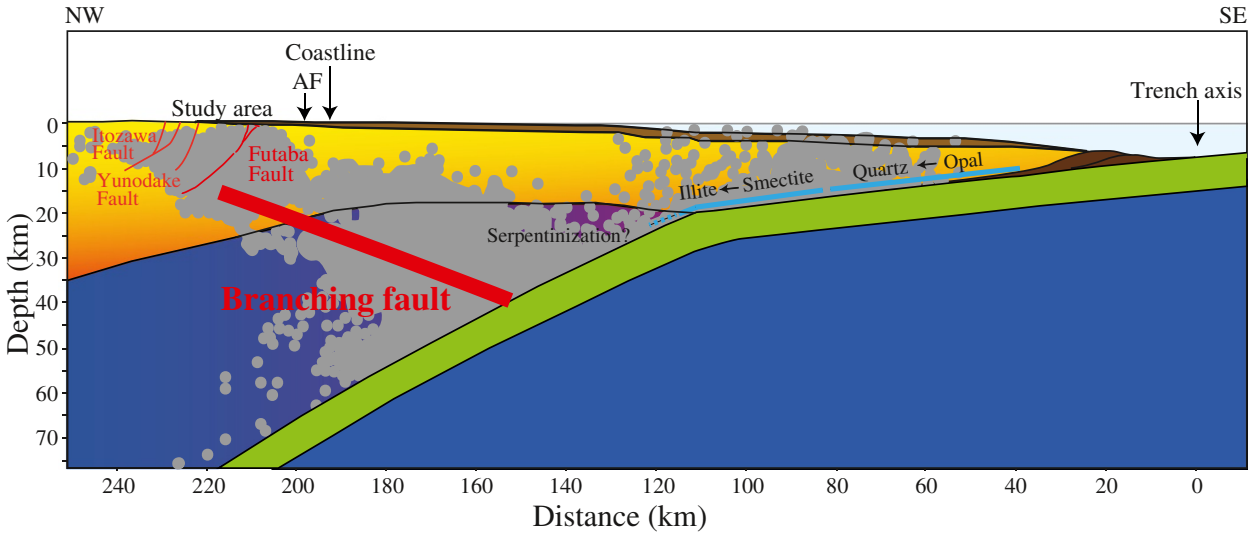

Figure 6 Schematic figure of subduction zone in the southern part of the Japan Trench. The figure is constructed based on Figures ten panel a and fifteen of Miura et al. (2003) and Figure four of Tsuru et al. (2002) by expanding the original figure landward and depthward. Microearthquakes (gray circles) in the overlying plate and a branching fault (thick red line) are shown based on Imanishi et al. (2012). Active faults and coseismic faults during the 2011 Iwaki Earthquake are shown in red (Fukushima et al. 2013). The trace of the Futaba Fault is drawn using a dipping angle and depth extent as determined by a recent seismic survey by Sato et al. (2013). The depth ranges for opal to quartz and smectite to illite transitions were drawn after Kimura et al. (2012). AF denotes the aseismic front after Yoshii (1975, 1979).

According to Kazahaya et al. (2014, Figure two panel B), the end-member of Arima-type deep-seated fluids in southwest Japan, which has been considered to be derived from the subducting Philippine Sea Plate, is within the range of magmatic gas in the δD to $\delta^{18}O$ diagram. The values of δD and $\delta^{18}O$ for our deep groundwater samples (Figure 2a) fall on the trends for altered seawater in their diagrams. In addition, our samples have lower Cl concentration than seawater, whereas the Cl concentration of Arima-type deep-seated fluids is more than 4 wt.% (Kazahaya et al. 2014). It should be emphasized that the δD, $\delta^{18}O$, and Cl data of our samples do not have Arima-type deep-seated fluid characteristics, although they might have migrated through the mantle wedge. One possible cause of the difference is the difference in temperature between the Nankai Trough and Japan Trench; that is, the calculated temperature along the slab/mantle interface at a depth of 50 km is only 200°C in northeast Japan (Peacock and Wang 1999). More detailed geochemical investigations need to be undertaken to determine the origin of iodine and fluid-flow paths in the Tohoku subduction zone. The Joban and Hamadori area, where we sampled deep groundwater from basement rocks, may be a good window to look into the fluid circulation in a subduction zone related to subducted sediments.

Conclusions

We measured δD, $\delta^{18}O$, $^{129}I/I$, $^{36}Cl/Cl$, and ^{3}H concentrations in deep groundwater in the Joban and Hamadori areas in southern Tohoku and inferred the origin of iodine contained in the water. Main results are summarized as follows:

(1) The hypothetical end-member of the groundwater, estimated from the relationship between Cl and $\delta^{18}O$, revealed much higher iodine and lower Cl concentrations in the groundwater than those in seawater. The I and Cl concentrations can be explained by the mixing of the hypothetical end-member, meteoric water, and seawater.

(2) Ages of iodine in deep groundwater from the Joban and Hamadori areas were uniform and were approximately 40 Ma. Most of the $^{36}Cl/Cl$ ratios were within a range of the secular equilibrium.

(3) The I/Cl ratio of the deep groundwater increases with increasing temperature. The temperature of the groundwater is high with a maximum of 78°C at a depth of 1,100 m, and the groundwater in the Joban basin is unlikely to be a source of the groundwater in the study areas because the geothermal gradient (18°C km^{-1}) of the basin is low. Basement rocks in the study areas are older than Cretaceous and cannot be a source of the iodine either.

(4) Subducted sediments in the Japan Trench are a possible source of iodine in the groundwater because the sediments in the northwestern Pacific Ocean contain organic carbon as much as 0.5 to 1.0 wt.%. Active faults are developed in the study area and a large amount of groundwater was discharged during and after the 2011 Iwaki earthquake.

Microseismicity was also recognized from the subducted plate all the way to the study area after the 2011 Tohoku-oki earthquake. Those results and the iodine ages suggest that the groundwater migrated through fractured basement rocks from the subduction plate to the study areas at a rate of 2 to 5 mm year^{-1}.

Additional file

Additional file 1: Table S1. Major and trace element compositions of representative rock samples. Data for rocks similar to the host rocks of our sampling locations were selected from the original data reported in Morikawa and Tosaki (2013).

Competing interests
The authors declare that they have no competing interests.

Authors' contributions
YST carried out the measurements of iodine concentrations and ^{129}I/I ratios and drafted the initial manuscript. KK coordinated the present work and helped YST to complete the manuscript. YT and NM determined ^{36}Cl/Cl, HM performed the AMS measurements, MT carried out the ion chromatography and stable isotope analyses, and TS participated in the groundwater sampling. All authors read and approved the final manuscript.

Acknowledgements
This study was funded by a Grant-in-Aid for Scientific Research on Innovative Areas, specifically, 'Geofluids: Nature and dynamics of fluids in subduction zones' from the Ministry of Education, Culture, Sports, Science, and Technology, Japan (No. 24109706). The authors sincerely thank K. Sasa and T. Takahashi (University of Tsukuba Tandem Accelerator Complex) for measuring ^{36}Cl/Cl.

Author details
[1]Institute of Earthquake and Volcano Geology, National Institute of Advanced Industrial Science and Technology (AIST), 1-1-1 Higashi, Tsukuba, Ibaraki 305-8567, Japan. [2]Department of Nuclear Engineering and Management, School of Engineering, The University of Tokyo, 2-11-16 Yayoi, Bunkyo-ku, Tokyo 113-0032, Japan.

Received: 19 November 2013 Accepted: 19 September 2014
Published: 20 October 2014

References
Andrews JN, Fontes J-Ch, Michelot J-L, Elmore D (1986) In-situ neutron flux, ^{36}Cl production and groundwater evolution in crystalline rocks at Stripa, Sweden. Earth Planet Sci Lett 77:49–58

Chester FM, Rowe C, Ujiie K, Kirkpatrick J, Regalla C, Remitti F, Moore JC, Toy V, Wolfson-Schwehr M, Bose S, Kameda J, Mori JJ, Brodsky EE, Eguchi N, Toczko S, Expedition 343 and 343T Scientists (2013) Structure and composition of the plate-boundary slip zone for the 2011 Tohoku-oki earthquake. Science 342:1208–1211

Clayton RN, Friedman I, Graf DL, Mayeda TK, Meents WF, Shimp NF (1966) The origin of saline formation waters 1. Isotopic composition. J Geophys Res 71:3869–3882

Dansgaard W (1964) Stable isotopes in precipitation. Tellus 16:436–468

Elderfield H, Truesdale VW (1980) On the biophilic nature of iodine in seawater. Earth Planet Sci Lett 50:105–114

Faulkner DR, Rutter EH (2000) Comparisons of water and argon permeability in natural clay-bearing fault gouge under high pressure at 20°C. J Geophys Res 105:16415–16426

Fehn U (2012) Tracing crustal fluids: applications of natural ^{129}I and ^{36}Cl. Annu Rev Earth Planet Sci 40:45–67

Fehn U, Snyder G, Egeberg PK (2000) Dating of pore waters with ^{129}I: relevance for the origin of marine gas hydrates. Science 289:2332–2335

Fehn U, Snyder GT, Matsumoto R, Muramatsu Y, Tomaru H (2003) Iodine dating of pore waters associated with gas hydrates in the Nankai area, Japan. Geology 31:521–524

Fehn U, Moran JE, Snyder GT, Muramatsu Y (2007a) The initial ^{129}I/I ratio and presence of 'old' iodine in continental margins. Nuc Inst Meth Phys Res B 259:496–502

Fehn U, Snyder GT, Muramatsu Y (2007b) Iodine as a tracer of organic material: ^{129}I results from gas hydrate systems and fore arc fluid. J Geochem Explor 95:66–80

Fifield LK, Tims SG, Fujioka T, Hoo WT, Everett SE (2010) Accelerator mass spectrometry with the 14UD accelerator at the Australian National University. Nucl Instrum Meth Phys Res B 268:858–862

Fifield LK, Tims SG, Stone JO, Argento DC, Cesare MDe (2013) Ultra-sensitive measurements of ^{36}Cl and ^{236}U at the Australian National University. Nucl Instrum Meth Phys Res B 294:126–131

Fukushima Y, Takada Y, Hashimoto M (2013) Complex ruptures of the 11 April 2011 M_w 6.6 Iwaki earthquake triggered by the 11 March 2011 M_w 9.0 Tohoku earthquake, Japan. Bull Seismol Soc Am 103:1572–1583

Geochemical Earth Reference Model (2014), EarthRef. org. http://EarthRef.org/. Accessed 05 May 2014

GeomapNavi (2014) Geological survey of Japan, National Institute for Advanced Industrial Science and Technology., https://gbank.gsj.jp/geonavi/. Accessed 25 Apr 2014

Hiroi Y, Kishi S, Nohara T, Sato K, Goto J (1998) Cretaceous high-temperature rapid loading and unloading in the Abukuma metamorphic terrane, Japan. J Metamorphic Geol 16:67–81

Imanishi K, Ando R, Kuwahara Y (2012) Unusual shallow normal-faulting earthquake sequence in compressional northeast Japan activated after the 2011 off the Pacific coast of Tohoku earthquake. Geophys Res Lett 39, L09306

Inaba T, Sampei Y, Nagamatsu T, Yonekura Y (2009) Petroleum source-rock potential of the Cretaceous marine argillaceous rocks in the offshore Joban fore-arc Basin, northeast Japan. J Jpn Assoc Petrol Technol 74:560–572 [in Japanese with English abstract]

Inamura A, Yasuhara M (2003) Hydrogen and oxygen isotopic ratios of river water in the Kanto Plain and surrounding mountainous regions, Japan. J Jpn Assoc Hydrol Sci 33:115–124 [in Japanese with English abstract]

Iwata T, Hirai A, Inaba T, Hirano M (2002) Petroleum system in the offshore Joban Basin, northeast Japan. J Jpn Assoc Petrol Technol 67:62–71 [in Japanese with English abstract]

Japan Meteorological Agency (2011) Earthquake information., http://www.data.jma.go.jp/svd/eqdb/data/shindo/index.php. Accessed 15 Apr 2014

Japan Meteorological Agency (2013) Daily surface seawater temperature in and around Japan., http://www.data.jma.go.jp/gmd/kaiyou/data/db/kaikyo/daily/t100_jp.html. Accessed 13 Jan 2014

Kasai K (2008) Hot springs and geology of Ibaraki: exploration of heat source of hot springs from geological structures. Ibaraki Hot Spring Developer, Co. Ltd, Mito [in Japanese]

Kazahaya K, Sato T, Takahashi M, Tosaki Y, Morikawa N, Takahashi H, Horiguchi K (2013) Genesis of thermal water related to Iwaki-Nairiku earthquake. In: Japan Geoscience Union Meeting, Makuhari Messe, Chiba, 19–24 May 2013

Kazahaya K, Takahashi M, Yasuhara M, Nishio Y, Inamura A, Morikawa N, Sato T, Takahashi HA, Kitaoka K, Ohsawa S, Oyama Y, Ohwada M, Tsukamoto H, Horiguchi K, Tosaki Y, Kirita T (2014) Spatial distribution and feature of slab-related deep-seated fluid in SW Japan. J Jpn Assoc Hydrol Sci 44:3–16 [in Japanese with English abstract]

Kimura G, Hina S, Hamada Y, Kameda J, Tsuji T, Kinoshita M, Yamaguchi A (2012) Runaway slip to the trench due to rupture of highly pressurized megathrust beneath the middle trench slope: the tsunamigenesis of the 2011 Tohoku earthquake off the east coast of northern Japan. Earth Planet Sci Lett 339–340:32–45

Klauda JB, Sandler SI (2005) Global distribution of methane hydrate in ocean sediment. Energy Fuels 19:459–470

Kobayashi T, Tobita M, Koarai M, Okatani T, Suzuki A, Noguchi Y, Yamanaka M, Miyahara B (2012) InSAR-derived crustal deformation and fault models of normal faulting earthquake (M_j 7.0) in the Fukushima-Hamadori area. Earth Planets Space 64:1209–1221

Kwon O, Kronenberg AK, Gangi AF, Johnson B, Herbert BE (2004a) Permeability of illite-bearing shale: 1. Anisotropy and effects of clay content and loading. J Geophys Res 109, B10205

Kwon O, Herbert BE, Kronenberg AK (2004b) Permeability of illite-bearing shale: 2. Influence of fluid chemistry on flow and functionally connected pores. J Geophys Res 109, B10206

Mahara Y, Ohta T, Tokunaga T, Matsuzaki H, Nakata E, Miyamoto Y, Mizuochi Y, Tashiro T, Ono M, Igarashi T, Nagao K (2012) Comparison of stable isotopes, ratios of ^{36}Cl/Cl and ^{129}I/^{127}I in brine and deep groundwater from the Pacific coastal region and the eastern margin of the Japan Sea. App Geochem 27:2389–2402

Martin JB, Gieskes JM, Torres M, Kastner M (1993) Bromine and iodine in Peru margin sediments and pore fluids: implications for fluid origins. Geochim Cosmochim Ac 57:4377–4389

Matsuzaki H, Muramatsu Y, Kato K, Yasumoto M, Nakano C (2007) Development of ^{129}I-AMS system at MALT and measurements of ^{129}I concentrations in several Japanese soils. Nucl Instr Meth Phys Res B 259:721–726

Miura S, Kodaira S, Nakanishi A, Tsuru T, Takahashi N, Hirata N, Kaneda Y (2003) Structural characteristics controlling the seismicity of southern Japan Trench fore-arc region, revealed by ocean bottom seismographic data. Tectonophysics 363:79–102

Moran JE, Fehn U, Teng RTD (1998) Variations in ^{129}I/^{127}I ratios in recent marine sediments: evidence for a fossil organic component. Chem Geol 152:193–203

Morgenstern U, Taylor CB (2009) Ultra low-level tritium measurement using electrolytic enrichment and LSC. Isot Environ Health Stud 45:96–117

Morikawa N, Tosaki Y (2013) Data set of the helium isotope production ratios and the secular equilibrium values of chlorine-36 isotopic ratios (^{36}Cl/Cl) for the aquifer rocks in the Japanese islands: towards the improvement of the dating methods for old groundwaters. Open-file report of the geological survey of Japan. AIST 582:1–21, [in Japanese with English abstract]

Muramatsu Y, Wedepohl KH (1998) The distribution of iodine in the earth's crust. Chem Geol 147:201–216

Muramatsu Y, Fehn U, Yoshida S (2001) Recycling of iodine in fore-arc areas: evidence from the iodine brines in Chiba, Japan. Earth Planet Sci Lett 192:583–593

Muramatsu Y, Takada Y, Matsuzaki H, Yoshida S (2008) AMS analysis of ^{129}I in Japanese soil samples collected from background areas far from nuclear facilities. Quat Geochronol 3:291–297

Peacock SM, Wang K (1999) Seismic consequences of warm versus cool subduction metamorphism: examples from southwest and northeast Japan. Science 286:937–939

Premuzic ET, Benkovitz CM, Gaffney JS, Walsh JJ (1982) The nature and distribution of organic matter in the surface sediments of world oceans and seas. Org Geochem 4:63–77

Sasa K, Takahashi T, Tosaki Y, Matsushi Y, Sueki K, Tamari M, Amano T, Oki T, Mihara S, Yamato Y, Nagashima Y, Bessho K, Kinoshita N, Matsumura H (2010) Status and research programs of the multinuclide accelerator mass spectrometry system at the University of Tsukuba. Nucl Instr Meth Phys Res B 268:871–875

Sato T, Kazahaya K, Yasuhara M, Itoh J, Takahashi HA, Morikawa N, Takahashi M, Inamura A, Handa H, Matsumoto N (2011) Hydrological changes due to the M7.0 earthquake at Iwaki, Fukushima induced by the 2011 Tohoku-oki earthquake, Japan. In: American Geophysical Union, Fall Meeting. The Moscone Center, San Francisco, 5–9 December 2011

Sato H, Ishiyama T, Kato N, Higashinaka M, Kurashimo E, Iwasaki T, Abe S (2013) An active footwall shortcut thrust revealed by seismic reflection profiling: a case study of the Futaba fault, northern Honshu, Japan. EGU General Assembly, Austria Center, Vienna, 07–12 April 2013

Sharma P, Bourgeois M, Elmore D, Granger D, Lipschutz ME, Ma X, Miller T, Mueller K, Rickey F, Simms P, Vogt S (2000) PRIME lab AMS performance, upgrades and research applications. Nucl Instrum Meth Phys Res B 172:112–123

Shibata T, Nakamura E (1997) Across-arc variations of isotope and trace element compositions from quaternary basaltic volcanic rocks in northeastern Japan: implications for interaction between subducted oceanic slab and mantle wedge. J Geophys Res 102:8051–8064

Shipboard Scientific Party (1980) DSDP volume LVI and LVII table of contents. site 436, Japan Trench Outer Rise, leg 56, doi:10.2973/dsdp.proc.5657.107.1980

Sibson RH (1992) Implications of fault-valve behaviour for rupture nucleation and recurrence. Tectonophysics 211:283–293

Sibson RH (2013) Stress switching in subduction forearcs: implications for overpressure containment and strength cycling on megathrusts. Tectonophysics 600:142–152

Snyder GT, Fabryka-Martin JT (2007) ^{129}I and ^{36}Cl in dilute hydrocarbon waters: marine-cosmogenic, in situ, and anthropogenic sources. Appl Geochem 22:692–714

Snyder G, Fehn U (2004) Global distribution of ^{129}I in rivers and lakes: implications for iodine cycling in surface reservoirs. Nucl Instrum Meth Phys Res B 223–224:579–586

Tagami K, Uchida S (2006) Concentrations of chlorine, bromine and iodine in Japanese rivers. Chemosphere 65:2358–2365

Takahashi M, Kazahaya K, Yasuhara M, Takahashi HA, Morikawa N, Inamura A (2004) Geochemical study of hot spring waters in Abukuma area, northeast Japan. J Jpn Assoc Hydrol Sci 34:227–244 [in Japanese with English abstract]

Tanaka A, Yano Y, Sasada M, Yamano M (2004) Geothermal gradient and heat flow data in and around Japan. Geological Survey of Japan (CD-ROM database)

The Research Group for Active Faults of Japan (1991) Active faults in Japan (Sheet Maps and Inventories), revised edn. University of Tokyo Press, Tokyo, p 163

Toda S, Tsutsumi H (2013) Simultaneous reactivation of two, subparallel, inland normal faults during the M_w 6.6 11 April 2011 Iwaki earthquake triggered by the M_w 9.0 Tohoku-oki, Japan, earthquake. Bull Seismol Soc Am 103:1584–1602

Tokyo Electric Power Company (2012) Fukushima First and Second Nuclear Power Plants; geology and geological structures of the power plant sites. Tokyo Electric Power Company, http://www.tepco.co.jp/cc/direct/images/120810d.pdf Accessed 30 Apr 2014 [in Japanese]

Tomaru H, Ohsawa S, Amita K, Lu Z, Fehn U (2007a) Influence of subduction zone settings on the origin of forearc fluids: halogen concentrations and ^{129}I/I ratios in waters from Kyushu, Japan. Appl Geochem 22:676–691

Tomaru H, Lu Z, Fehn U, Muramatsu Y, Matsumoto R (2007b) Age variation of pore water iodine in the eastern Nankai Trough, Japan: evidence for different methane sources in a large gas hydrate field. Geology 35:1015–1018

Tomaru H, Lu Z, Snyder GT, Fehn U, Hiruta A, Matsumoto R (2007c) Origin and age of pore waters in an actively venting gas hydrate field near Sado Island, Japan Sea: interpretation of halogen and ^{129}I distributions. Chem Geol 236:350–366

Tomaru H, Fehn U, Lu Z, Takeuchi R, Inagaki F, Imachi H, Kotani R, Matsumoto R, Aoike K (2009a) Dating of dissolved iodine in pore waters from the gas hydrate occurrence offshore Shimokita Peninsula, Japan: ^{129}I results from the D/V Chikyu shakedown cruise. Resour Geol 59:359–373

Tomaru H, Lu Z, Fehn U, Muramatsu Y (2009b) Origin of hydrocarbons in the Green Tuff region of Japan: ^{129}I results from oil field brines and hot springs in the Akita and Niigata Basins. Chem Geol 264:221–231

Tomita T, Ohtani T, Shigematsu N, Tanaka H, Fujimoto K, Kobayashi Y, Miyashita Y, Omura K (2002) Development of the Hatagawa Fault Zone clarified by geological and geochronological studies. Earth Planets Space 54:1095–1102

Tosaki Y, Tase N, Kondoh A, Sasa K, Takahashi T, Nagashima Y (2011) Distribution of ^{36}Cl in the Yoro River basin, central Japan, and its relation to the residence time of the regional groundwater flow system. Water 3:64–78

Tsuru T, Park J-O, Miura S, Kodaira S, Kido Y, Hayashi T (2002) Along-arc structural variation of the plate boundary at the Japan Trench margin: implication of interplate coupling. J Geophys Res 107(B12):2357, doi:10.1029/2001JB001664

Uehara S, Shimamoto T (2004) Gas permeability evolution of cataclasite and fault gouge in triaxial compression and implications for changes in fault-zone permeability structure through the earthquake cycle. Tectonophysics 378:183–195

von Huene R, Culotta R (1989) Tectonic erosion at the front of the Japan Trench convergent margin. Tectonophysics 160:75–90

von Huene R, Lallemand S (1990) Tectonic erosion along the Japan and Peru convergent margins. Geol Soc Am Bull 102:704–720

Yanagisawa Y, Nakamura K, Suzuki Y, Sawamura K, Yoshida F, Tanaka Y, Honda Y, Tanahashi M (1989) Tertiary biostratigraphy and subsurface geology of the Futaba district, Joban Coalfield, northeast Japan. Bull Geol Surv Japan 40 (8):405–467 [in Japanese with English abstract]

Yoshii T (1975) Proposal of the "aseismic front". Zisin 2(28):365–367 [in Japanese]

Yoshii T (1979) A detailed cross-section of the deep seismic zone beneath northeastern Honshu, Japan. Techtonophysics 55:349–360

doi:10.1186/1880-5981-66-131
Cite this article as: Togo *et al.*: **Groundwater, possibly originated from subducted sediments, in Joban and Hamadori areas, southern Tohoku, Japan.** *Earth, Planets and Space* 2014 **66**:131.